Biophysics

Review

Twisting and extension: Application of magnetic tweezers to DNA studies

Arsha Moorthy[1], Alireza Sarvestani[2], Whitney Massock[1] and Chamaree de Silva[1,*]

[1] College of Liberal Arts and Sciences, Mercer University, Macon, GA 31207, USA

[2] School of Engineering, Mercer University, Macon, GA 31207, USA

* **Correspondence:** Email: desilva_c@mercer.edu; Tel: +14783012770.

Abstract: Magnetic tweezers have emerged as a vital force spectroscopy tool for characterizing the mechanical properties of nucleic acids and their interactions with proteins. Harnessing the principles of magnetic theory, magnetic tweezers allow for the precise manipulation of biological compounds at the single-molecule level through the imposition of a magnetic field. This review focuses on the application of magnetic tweezers in the context of DNA studies, with a particular emphasis on the mechanical properties of DNA and its dynamic interactions with proteins and enzymes. These interactions are essential to genomic transactions such as DNA replication, repair, and transcription. Over the last few decades, magnetic tweezer technology has experienced significant advancements, leading to the development of different types of magnetic tweezers. These technological breakthroughs have opened up new avenues of scientific research, including studies related to DNA elasticity, supercoiling, replication, and repair.

Keywords: magnetic tweezers; DNA; magnetic theory; DNA supercoiling; DNA transcription; DNA replication; force spectroscopy

1. Introduction

Force-based micromanipulation of biological molecules is an important technique to characterize the effects of mechanical stimuli at the single-molecule level. Optical tweezers (OTs) are one of the first force spectroscopy techniques in which a laser beam focused through an objective lens is used to move, trap, or apply forces to molecules [1]. Parallel to the development of OTs, scientists began to explore other avenues of non-invasive micromanipulation of biological molecules. In 1949, prior to discovering the structure of DNA, Crick and Hughes were probably the first to apply magnetic forces to single cells by allowing them to phagocytize magnetic particles and then manipulating these cells using an external magnetic field [2]. While the technique utilized by Crick and Hughes was crude and subject to several limitations, the magnetic particle phagocytosis created strides in understanding cell
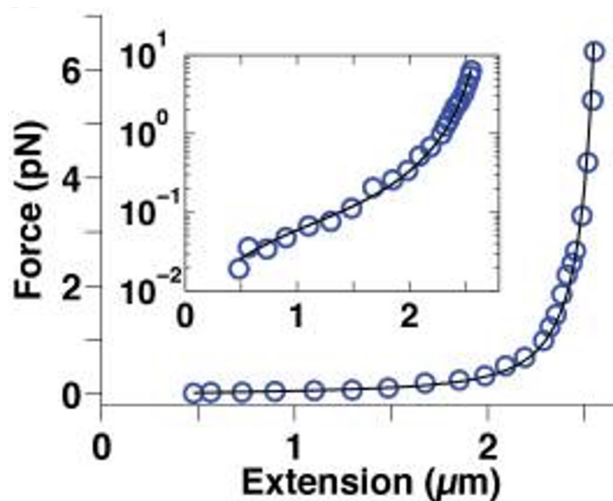
cytoplasmic rheology and structure [3, 4].

Figure 1. Variation of force with extension for a 7.9 kb DNA molecule. The solid line shows the prediction of WLC model with contour length 2,710 nm and persistence length 45 nm. Adapted from Lipfert et al. [5].

In 1992, Smith et al. [6] revolutionized the application of magnetic theory to explore biological systems by using magnetic beads to apply forces on individual DNA molecules. The DNA molecules were attached to a coverslip on one end and to a paramagnetic bead on the other end. The setup was housed in a microflow chamber and DNA molecules were stretched by the buffer flow parallel to the glass surface, whereas the magnetic field was applied normal to the flow direction. By tracking the bead position at different flow rates, they obtained the relation between the resultant external force and DNA extension. Their results and all subsequent measurements by others revealed two distinct regions in force-extension curves of DNA: an initial linear followed by a nonlinear response where the curve deviates from the linear region due to the maximum extensibility of DNA [7]. These observations are in close agreement with the predictions of the worm-like chain (WLC) model for semi-flexible molecules (Figure 1) [8]. The experimental results of Smith et al. [6] confirmed the existence of a significant local curvature in the structure of DNA. While this technique laid the ground for a better understanding of DNA micromechanics, it was subjected to certain limitations, such as increased viscous drag endured by the magnetic beads, resulting from the parallel extension of DNA along the coverslip [9].

Strick et al. [10] eliminated the use of a flow chamber by applying an upward force, perpendicular to the coverslip, that was generated by magnets. In their experimental setting, the individual DNA molecule was housed in a microchamber with a pair of permanent magnets directly above it. The individual DNA molecule was labeled with biotin and digoxigenin at its extremities and was bound to a streptavidin coated paramagnetic bead on one end and tethered to an anti-digoxigenin-coated glass surface on the other end. The magnetic field was used to rotate the bead to coil and pull the DNA molecule perpendicular to the coverslip (Figure 2). Strick's assay has come to be termed the *conventional* magnetic tweezers (MTs). The position of the bead is measured in 3D using a computerized image that detects changes in the bead's vertical and horizontal positions. A light

source is placed above the microscope and an image of the bead is created using a charged-coupled device camera. Many modifications have since been made to MTs to enhance the resiliency of tethered DNA at higher forces, control of DNA topology, and bead-tracking resolution [11–18].
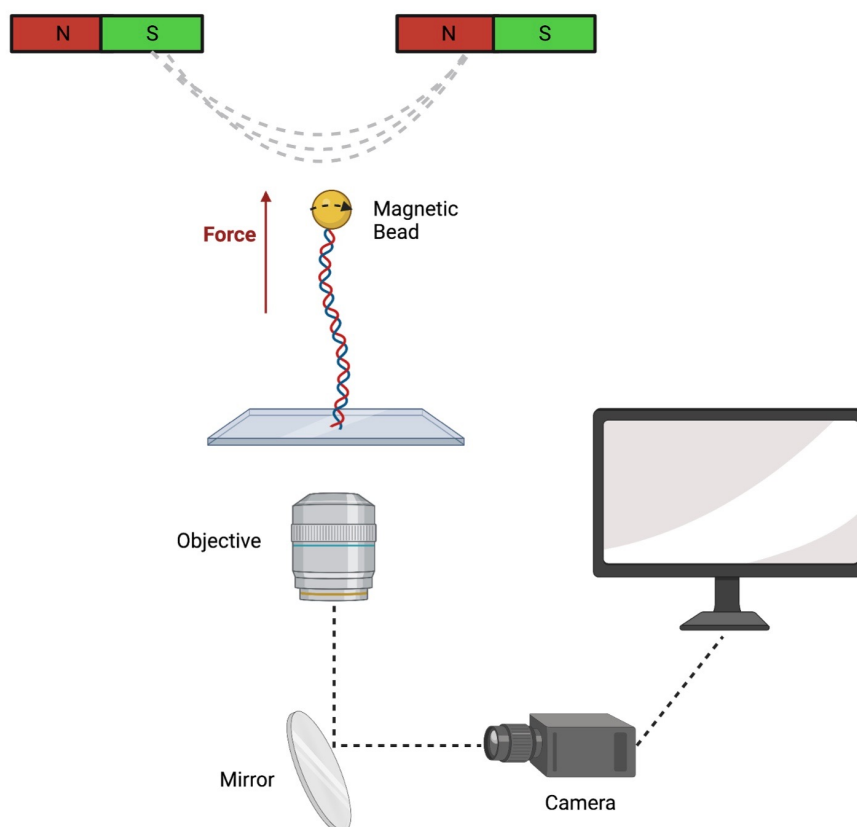

Figure 2. Schematic structure of conventional MTs. A pair of permanent magnets (red and green) is used to produce a magnetic field (dashed lines). The superparamagnetic bead (yellow) is attached to a DNA that is tethered to a coverslip on the opposite side. The generated magnetic field pulls the bead in the direction of the field gradient and pulls the DNA molecule. The magnetic force can be adjusted by moving the magnets vertically up and down. The magnets can be rotated, which in turn twist the DNA molecule. A microscope objective allows for the bead to be imaged onto a camera and a computer for real-time position tracking.

2. Types of magnetic tweezers

Multiple types of MTs have been invented and used, including (1) permanent MTs that use permanent magnets to generate a magnetic field to pull and twist superparamagnetic beads [19], (2) electromagnetic tweezers where the magnetic field is generated by an electromagnet [20], (3) hybrid MTs that combine permanent magnets with ferromagnetic pole materials for enhanced control over magnetic particles [21], and (4) magnetic-optical tweezers that utilize a combination of magnetic and optical forces to manipulate magnetic particles [22]. In what follows, different configurations of

permanent MTs are explained.

2.1. Conventional magnetic tweezers

MTs function as force clamps, enabling precise control over the force applied to a molecule, rather than fixing its extension. With conventional MTs, force can only be applied vertically to the bead, allowing the DNA molecule to be pulled upwards in varying degrees of extension (Figure 2). Conventional MTs can also operate in angular position clamp mode by applying a torque and clamping the angular orientation of the beads. Prior to applying force or torque, it must be ensured that the DNA is free of nicks and possesses the proper multi-labeled binding on both ends. One end of the DNA is functionalized with digoxigenin (dig handle) and is attached to an anti-dig-coated coverslip. The other end of the DNA is functionalized with biotin (bio handle), which attaches to a streptavidin-coated paramagnetic bead. Magnetic tweezing measurements on DNA are typically performed in a buffer solution. TE(TE is a widely recognized buffer solution, and it is always denoted as "TE" in technical documents. The T and E stand for Tris-HCL and EDTA, respectively) tethering buffer is one of the most commonly used buffer solutions that contains Tris-HCl, EDTA, and NaCl [5]. The horizontal magnetic field is created using a pair of cubic magnets, in which the force between the magnets and the bead can be controlled by changing the distance between the two. The magnetic field keeps the bead in place, constraining its Brownian motion. The stationary position of the bead allows the magnets to be rotated, which in turn rotates the bead and twists the DNA. The average extension of the DNA can be found by tracing the vertical position of the bead along the z-axis. By modeling the DNA-bead system as a *small pendulum*, the stretching force applied to the bead can be determined by analyzing its Brownian fluctuations [23]. The experiments can be performed on different types of nucleic acids, as well as different nucleoprotein complexes [24].

While conventional MTs provide a quick and relatively easy approach for torque estimations, their applications are limited to measuring relatively large torques [25]. They have a limited torque resolution, unsuitable for biological torque measurements that require a resolution of 10 pN.nm or better [26]. To achieve biologically relevant torque measurements, it becomes essential to either use larger beads (which significantly increase the measurement time) or use different types of MTs with smaller rotational trap stiffness.

2.2. Freely-orbiting magnetic tweezers

Unlike conventional MTs, freely-orbiting MTs (FOMTs) do not constrain the rotational motion of DNA, giving the ability to measure twists in DNA at high resolutions. This design utilizes cylindrical magnets placed above the DNA-bead attachment to generate magnetic field lines that are vertically aligned with the tether's axis (Figure 3). Similar to conventional MTs, the force between the magnet and the bead can be varied by changing the distance between them. The absence of a horizontal magnetic field allows the bead to move along the horizontal xy-plane, since the position of the bead is only constrained by the DNA molecule (z-axis). Under these conditions, the bead undergoes Brownian fluctuations while moving in a circular annulus. The fluctuation is closely related to the rotation of the bead around its axis. The rotation angle and twist of the DNA molecule can be measured by tracking the bead's coordinates on the xy-plane. In order to obtain accurate measurements of the equilibrium position and fluctuations, a sufficient number of independent samples must be collected. Based on the

characteristic time scale of fluctuations, the measurement process may take several hours, depending on the size of the bead and DNA [27].
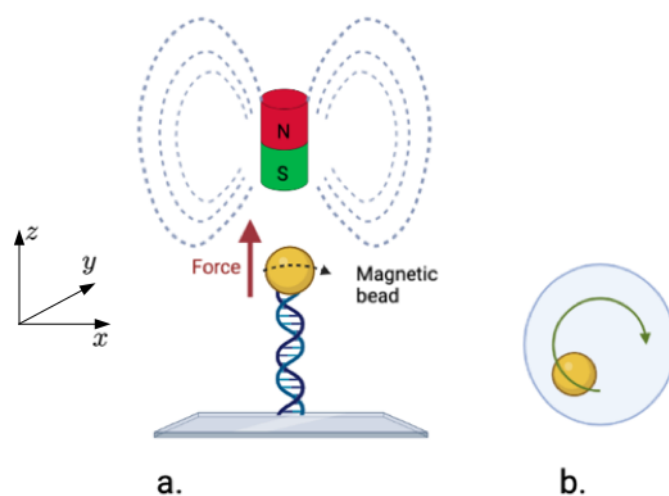

Figure 3. (a) A schematic representation of a tethered bead in FOMTs. Like other MTs, FOMTs consist of a DNA tethered on one end to a coverslip and on the other end to a superparamagnetic bead. A pair of cylindrical magnets (red and green) are placed above the assembly inducing a vertical magnetic field. (b) Aerial view of magnetic bead motion. In this model, the motion of the bead is unconstrained by the magnet, thus moving in a circular annulus.

The ability to measure DNA twists is important in understanding the assembly and helicity of nucleoprotein filaments during DNA repair. FOMTs were used to follow DNA unwinding during assembly of recombination protein A (RecA) filament on double-stranded DNA (dsDNA) [28]. RecA filaments are nucleoprotein complexes that serve as active intermediates during recombinational DNA repair [29]. RecA promotes the strand exchange between homologous DNA molecules by unwinding the dsDNA molecule. For example, Lipfert et al. [27] used FOMTs to show that RecA unwinds dsDNA through its helicase activity, which involves the binding of RecA to the dsDNA and formation of a nucleoprotein filament that stretches and separates the two strands. They showed that polymerization of RecA filaments outcompetes DNA re-hybridization and leads to a net extension of DNA after unwinding.

2.3. Magnetic torque tweezers

Magnetic torque tweezers (MTTs) are used to quantify the torsional properties of biological molecules by applying torque to them. Torque is applied by placing the DNA-bead in horizontal and vertical magnetic fields, generated by two sets of magnets (Figure 4). Cylindrical magnets produce a vertical magnetic field, while the small side magnets create a horizontal field. A vertical force is applied on the bead to attract it upwards in the vertical z-direction and a weak angular trap is applied to measure molecular torque from changes in the equilibrium angle. With FOMTs, the rotational fluctuations of the bead are solely constrained by the torsional stiffness of the DNA tether, rather than

being influenced by the magnets. With addition of a small horizontal field gradient to a strong vertical one, the bead position is more securely constrained. Constraining the bead motion makes it to move in a semicircle on the horizontal xy-plane. By tracking the angular fluctuation as a function of time, $\theta(t)$, with respect to a reference marker, the shift in the equilibrium angle induced by the external torque can be measured [30, 31]. The stiffness of the torsional trap, κ_θ, can be determined from the variance of angular fluctuations, σ_θ^2, as $\kappa_\theta = k_B T / \sigma_\theta^2$, where $k_B T$ is the thermal energy. The torque τ accumulated in the molecule after rotating by $\Delta\theta$ would be $\tau = \kappa_\theta \Delta\theta$. MTTs are used to gain information about DNA-protein and protein-protein interactions. Lipfert et al. [30], for example, studied the interactions of RecA filaments with DNA and discovered that RecA-DNA filaments have a much higher torsional stiffness than dsDNA alone.
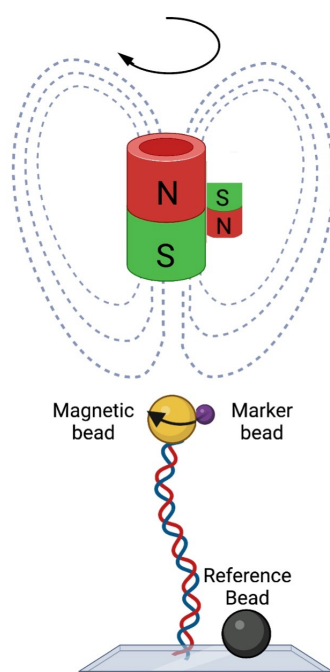

Figure 4. A schematic representation of a tethered bead in MTTs. This setup uses a pair of cylindrical magnets (large red and green) to create a vertical magnetic field and small side magnets (small red and green) to create a horizontal magnetic field. The combined magnetic fields apply forces and torque on the superparamagnetic bead (yellow) that is attached to the DNA molecule. A marker bead is attached to the magnetic bead. A reference bead is also placed in this field to help correct for drift.

Conventional MTs are capable of applying forces between 10 pN and 100 pN. A force less than 10 pN will cause the bead to be very close to the surface, at which point the interaction between the surface and the bead becomes comparable with the magnetic force. At forces greater than 100 pN, the majority of bonds used to tether the molecule become unstable [12]. Table 1 shows the maximum forces achieved considering different MTs and bead types. Different types of superparamagnetic beads are commercially available, including Dynabeads MyOne, Invitrogen M280, and Ademtech. In general, stronger forces can be applied by using larger beads or by reducing the separation of the magnets and the bead, however bigger beads generate greater drag forces (rotational drag coefficient scales with

the third power of the bead radius) and thus reduce the temporal resolution of experiments [5, 16]. Conventional MTs can measure the vertical displacements of beads with an accuracy of up to 10 nm [32], while in MTTs the tethered bead can be tracked with an accuracy of up to 5 nm [30]. The angular tracking algorithm of FOMTs, using cross-correlation analysis of radial section images, has an accuracy of 0.1° [27].

Calibration is required to determine the correct forces and torques from MTs measurements. There are two primary ways to calibrate MT [33]. The first method involves calculation of forces directly from the known magnetic field gradient. However, the practical application of this method may be limited due to the variability in bead size and magnetization density [34]. In the second approach, the force is extracted from the traced Brownian fluctuations of the beads [33–35]. This method, too, has its own limitations, particularly if the response time of short tethers is shorter than than the time that the camera shutter is open for data acquisition [36, 37]. Strategies to circumvent these limitations are explained elsewhere [33, 38].

Table 1. Maximum stretching forces achieved using different types of MTs and bead types. R shows the bead radius. Reproduced from Lipfert et al. [5].

Tweezing System	M270 (R=1.4 μm)	MyOne (R=0.5 μm)	Ademtech (R=0.25 μm)
Conventional MTs[a] (1 mm gap)	70 pN	8 pN	1.6 pN
FOMTs or MTTs[b] (2 mm diameter gap)	9 pN	1 pN	0.2 pN
FOMTs or MTTs[b] (1 mm diameter gap)	18 pN	2 pN	0.4 pN

[a] pair of cubic 5 mm magnets.
[b] stack of three cylindrical magnets, 6 mm diameter.

3. Applications of MTs to DNA studies

3.1. Study of DNA replication and transcription enzymes

In order for DNA to be correctly replicated and repaired, the coordinated actions of a variety of different enzymes are required to interact with the DNA [39–41]. During DNA replication, the hydrogen bonds between the complementary base-pars (bps) in dsDNA molecules are broken by helicase enzymes to expose the individual strands [42]. Topoisomerases bind to the DNA ahead of the fork to release the torsional strain. The released strands then act as templates for the synthesis of two new daughter strands. DNA polymerase enzymes then add new nucleotides to the new growing strands [43]. DNA repair mechanisms are essential for maintaining the integrity of the genome. Different types of DNA mutations can emerge that can be inherited or sporadically acquired throughout life [44]. The main pathways for DNA repair are [45] base excision repair [46], homologous recombination [47], nucleotide excision repair [48], mismatch repair [49], and non-homologous-end-joining [50]. These pathways involve various enzymes and proteins, such as topoisomerases, polymerases, and nucleases.

3.1.1. Supercoiling and topoisomerase

Supercoiling refers to the twisting of a dsDNA molecule around itself. Positive supercoiling or overwinding denotes the twisting of the molecule in the same right-handed direction as its helix. Alternatively, negative supercoiling refers to the twisting of the entire dsDNA molecule in the opposite left-handed direction, leading to the underwinding of the double helix. Supercoiling plays a vital role in various biological processes, including transcription, DNA replication and chromosomal segregation [51, 52]. MTs have significantly enhanced the quantitative analysis of supercoiling and the effect of enzymes on DNA supercoiling [17, 18, 28, 53].
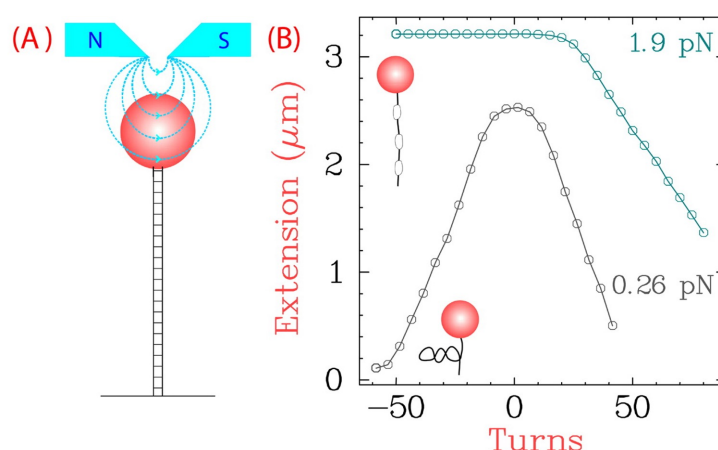

Figure 5. (A) Schematic illustration of a DNA molecule tethered between a substrate and a magnetic bead. Supercoils are formed by rotating the magnets. (B) Buckling of a twisted DNA molecule and formation of plectonemes at different extensions. At a sufficiently small tension ($F = 0.26$ pN), the DNA buckles at a small number of turns and the extension decreases symmetrically with increasing positive or negative supercoils. At higher force $F = 1.9$ pN, the DNA continues to contract as overwinding generates more supercoils. The buckling occurs only with positive rotations and DNA melts with underwinding. Adapted from Dekker et al. [54]. Copyright 2002 National Academy of Sciences.

Strick et al. [55] conducted one of the earliest studies on DNA supercoiling with MTs. They used conventional MTs to twist a DNA molecule and induce overwinding and underwinding at various stretching forces. Monitoring the motion of DNA tethers reveals how tension controls DNA supercoiling (Figure 5). Numerous studies have used this approach to study different aspects of supercoiling in different DNA constructs and using various types of MTs. The results generally show that when the tensile force is small, the torsional strain is built up by turning the molecule until a critical value at which it buckles to form plectonemic supercoils. As a result, the extension decreases symmetrically with increasing positive or negative supercoils. In the strong tension regime, DNA behavior varies depending on whether it is positively or negatively supercoiled. In the case of underwound DNA, the extension remains unaffected by the number of turns. This implies that DNA is not buckled, but instead is denatured [56]. For overwound DNA, it continues to contract by adding more plectonemes. This approach has enabled the examination of a diverse range of factors influencing the elasticity of supercoiled DNAs. For example, it has been shown that the elasticity of a

supercoiled DNA is highly influenced by the salinity of the solution [8, 24, 55, 57]. The overstretching transition force (force to stretch a DNA molecule to the halfway point of the transition width) increases as the ionic strength increases. For highly overwound DNA at sufficiently high salt concentrations, the chain extension depends on the previous history of DNA loading, indicating hysteresis behavior.
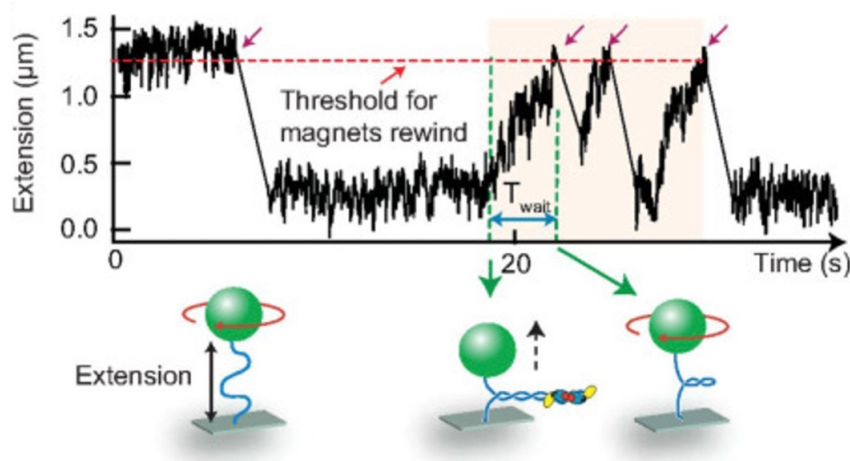

Figure 6. (A) A depiction of the experimental setup of MTs to study the relaxation of supercoiled DNA by topoisomerase. Pink arrows show the onset of supercoil formation with rotating magnets, followed by decreasing DNA extension. Upon addition of topoisomerase (green dashed lines) the supercoils are removed and extension reaches a threshold value (red dashed line). T_{wait} shows the mean wait time between introduction and complete relaxation of a fixed number of supercoils. Adapted from Seol et al. [58].

Topoisomerase enzymes mediate topological changes in DNA that are essential for DNA replication, transcription, and translocation. They do this by creating breaks in the DNA helix, relaxing torsional strain in supercoiled DNAs, and removal of catenanes and knots [59–61]. Topoisomerases transiently change DNA topology by cleaving the strands through transesterification reactions [62, 63]. Members of the topoisomerase superfamily are grouped into type I and II, each divided into subfamilies A and B [64]. Type I enzymes transiently cleave only one DNA strand, whereas type II enzymes cleave both strands [60]. MTs have contributed significantly to the understanding of the molecular details of topoisomerase functions in relaxation of supercoils [32, 65–69]. In a typical experiment, a DNA molecule is twisted by rotating the magnets (Figure 6). Past the buckling threshold, the DNA extension decreases due to plectoneme formation. Upon introduction of topoisomerases (and in the presence of ATP), the extension progressively increases concurrent with the removal of one plectonemic crossing [32, 54, 58, 70–76]. The process is reversible and by twisting the DNA, the supercoils can be regenerated.

Two types of type II topoisomerase are found in bacteria: DNA gyrase and topoisomerase IV (topo IV) [77]. DNA gyrase aids in new chain elongation during DNA replication, while topo IV separates daughter chromosomes that are linked topologically [77]. Specifically, DNA gyrase produces negative supercoils in the DNA, to counteract the positive supercoiling produced by the DNA duplex strands,

maintaining the negative DNA supercoiling ahead of the replication fork [73]. Unlike eukaryotic topoisomerases that relax positive and negative supercoils, prokaryotic topoisomerases discriminate between positive and negative supercoils. DNA gyrase actively generates negative and removes positive supercoils. Topo IV, on the other hand, preferentially relaxes positive supercoils. Using MTs, Crisona et al. [73] concluded that topo IV preferentially relaxes positive supercoils at 20 times the rate of relaxing negative supercoils, at low enzyme concentrations. The MTs setup allowed for the comparison of positive and negative supercoil relaxation in DNA at a given topo IV concentration. The chiral discrimination of topo IV, which prevents its interference with the winding activity of gyrase, has also been observed for relaxation of braided DNA. Chavin et al. [78] used MTs to show topo IV has a marked preference for the relaxation of left-handed braids.

Plectoneme formation and DNA supercoiling have been a subject of extensive theoretical investigations. Initial studies focused on ground state elastic models that did not consider entropic or electrostatic effects [79, 80]. Subsequent research incorporated entropic and electrostatic considerations [81]. In a major discovery, Rybenkov et al. [82] reported that topoisomerase IIA can decrease the fractions of knotted and linked DNA beyond the level expected at equilibrium thermodynamics. This explains why supercoil relaxation catalyzed by the enzyme relies on ATP hydrolysis. However, how a small enzyme can recognize the topology of a large DNA molecule remains elusive. Various models have been proposed to explain topology simplification by topoisomerases [83–85]. This includes DNA kinking [86], kinetic proofreading [87], three-segment binding [88], and the roles of hooked juxtapositions [89]. Although a comprehensive theory remains elusive, it is evident that the global characteristics of supercoiled DNA are directly influenced by local intra or intermolecular interactions between DNA segments. In particular, the juxtaposition of DNA double helices in crossover arrangements represents a ubiquitous motif in DNA structures [83]. Topoisomerases recognize underwound or overwound substrates by interacting preferentially with DNA crossovers [90]. A number of local properties of DNA–DNA juxtapositions may help topoisomerases discern global DNA topology. Electrostatics of DNA–DNA juxtapositions is the central player in regulation of these local properties [91, 92]. For example, the salinity-dependent elasticity of DNA is attributed to the electrostatic screening effect of ions and its effects on intermolecular interactions [91, 93].

3.1.2. Study of DNA helicase

Helicases play essential roles in DNA replication, repair, and recombination by unwinding dsDNA through NTP hydrolysis [94]. Acting as a motor protein, helicase translocates along the dsDNA and breaks the hydrogen bonds between the strands, causing their separation [95]. Helicases can be classified based on their stoichiometry (monomeric, dimeric, trimeric, or hexameric) in their active state or based on their function [96]. The functional classification depends on the polarity of translocation along the DNA strand. This is determined by the overhang required to initiate unwinding at the ss-dsDNA junction [97]. Helicases that move from the 3' to 5' direction are known as 3'–5' helicases, while those that move from the 5' to 3' direction are called 5'–3' helicases [98].

DNA-helicase interaction studies have significantly grown with MTs technology, allowing for the manipulation of force-induced mechanical changes to explore the mechanisms and functions of helicases. Croquette and co-workers [96, 99] utilized conventional MTs to monitor the unwinding of a singly nicked duplex DNA by UvrD, a member of the helicase superfamily present in *E. coli*. A

constant stretching force was applied to the DNA to induce unwinding bursts that were manifested by an increase in extension (Figure 7). The slope and height of the burst was used to determine multiple characteristics of the unwinding motor, such as mean processivity, unwinding rate, step size, and stoichiometry of ATP hydrolysis. The extension may instantaneously decrease back to the baseline, indicating rapid rehybridization of the two strands.
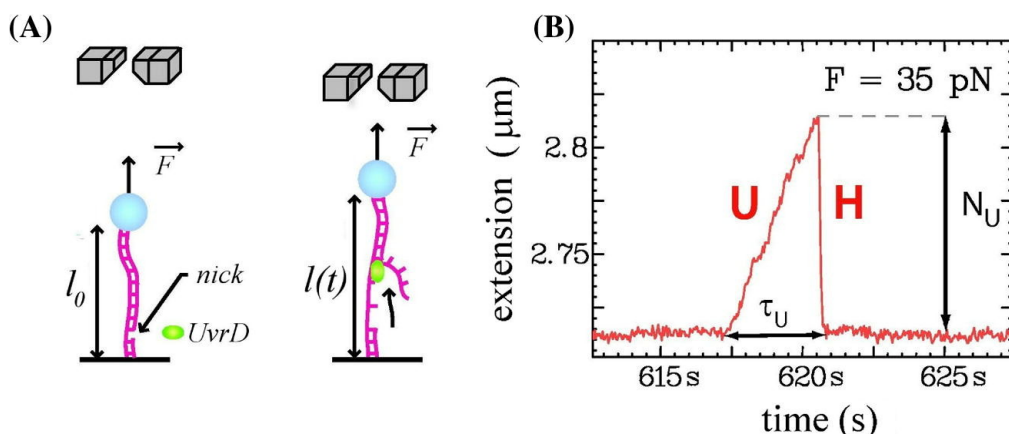

Figure 7. (A) UvrD helicase translocation by unwinding of a dsDNA. A nick on one strand serves as a loading site for the helicase. If the tension applied by the paramagnetic bead is sufficiently large ($F = 35$ pN), the rate of unwinding exceeds the rate of reannealing behind the complex and the extension of tethered ssDNA increases, as the helicase continues to unwind the strands. (B) Recorded extension vs time during unbinding **U** and rehybridization **H** of the two strands. By measuring the unbinding-induced extension N_U and unbinding time τ_U multiple characteristics of the unwinding motor such as mean processivity, unwinding rate, step size, and stoichiometry of ATP hydrolysis can be determined. Adapted from Hodeib et al. [96] with permission. Copyright 2016 Elsevier.

In an alternative setup, adding a hairpin to the DNA tether would enable the measurement of helicase unwinding activity through tracking the vertical position of the bead by analyzing the diffraction rings pattern in the bead image. By measuring the bead vertical position and, thus, the DNA extension over time, the authors could quantify the percentage of ssDNA created over time [95, 100, 101]. Sun et al. [102], for example, used conventional MTs to model DNA unwinding mechanisms induced by UvrD. The unwinding kinetics of UvrD was measured at various DNA-destabilizing forces. The DNA extension in their study showed unwinding followed by rehybridization or unwinding-rezipping patterns. More strikingly, they found that the force impeded the rate of helicase unwinding. Accordingly, the authors proposed the strained-inchworm model for which UvrD uses a strained inchworm mechanism to interpret the helicase-mediated unwinding of DNA.

3.1.3. Study of nuclease

Nucleases are essential to many DNA repair processes, such as base excision and mismatch repair, as they are responsible for breaking the phosphodiester bonds of the DNA bps [103]. DNA damage often leads to the formation of dsDNA breaks and failure to repair these breaks could lead to a

multitude of harmful effects, such as cancer predisposition and developmental defects [104]. Recent technological advancements have allowed researchers to examine the nuclease role in dsDNA breaks and repair. Carrasco et al. [104] utilized MTs to explore the nature of AddAB, a helicase-nuclease complex, specifically regarding the translocation that occurs during dsDNA break resection (Figure 8). By measuring the changes in the position of the superparamagnetic bead in a dsDNA with specific sequences with respect to time, they were able to calculate the velocity of DNA repair done by AddAB and the velocity that AddAB moved along the strand. Through this, they found that AddAB translational velocity decreased with the recognition of specific *cis* Chi (crossover hotspot instigator) sequences, with an observed increase in long pauses.
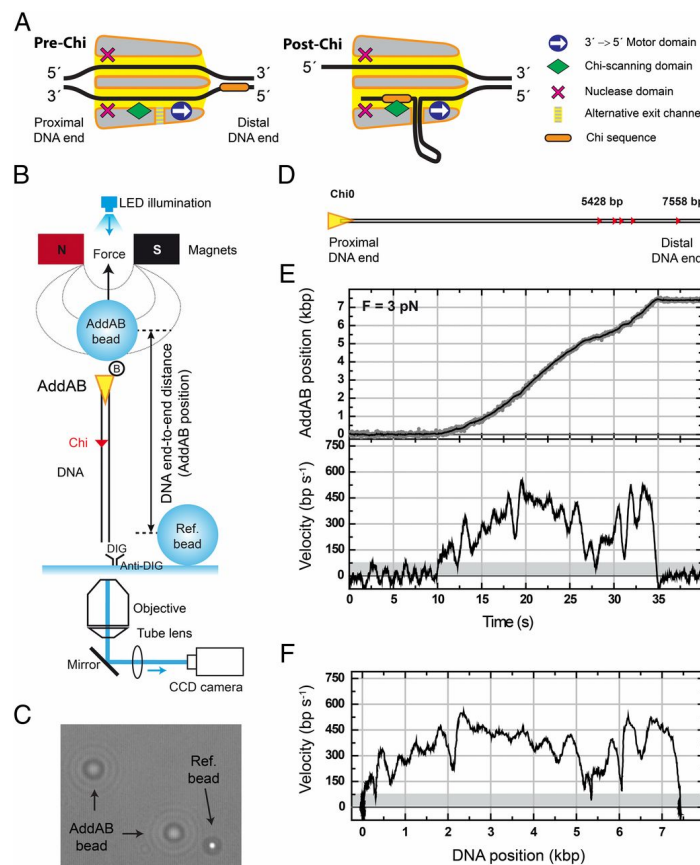

Figure 8. Translocation of AddAB complexes on single DNA molecules. (A) Schematic presentation of two ssDNA channels, the Chi-scanning module, 3'→5' ssDNA motor and the hypothetical alternative DNA exit channel positioned in between. (B) MTs setting used by Carrasco et al. [104] to quantify the dynamics of AddAB translocation. (C) AddAB beads and their positions relative to a reference bead. (D) The standard substrates used in the experiments consist of approximately 7500-bp DNA with a 5400-bp Chi-free section and five recombination hotspots at the distal end of the DNA. (E) An example of a complete AddAB translocation on a DNA subjected to 3 pN tension. The end-to-end distance was measured using the WLC model. (Upper) The time history AddAB position on the DNA. (Lower) The corresponding velocity of AddAB vs time. (F) The translocation velocity of AddAB as a function of its position. Adapted from Carrasco et al. [104].

Levikova et al. [105] investigated the helicase activity of DNA2, a nuclease-helicase involved with DNA metabolism in eukaryotes. In Saccharomyces cerevisiae, DNA2's nuclease activity was shown to be mandatory for all functions *in vivo*, while its less explored helicase function was reported to be weak. Through the use of MTs, they investigated the interaction between these 2 dynamic functions of DNA2, showing that DNA2's nuclease inhibits its helicase by cleaving 5 flaps that are required by the helicase domain to initiate substrate loading [105]. To examine the DNA2 helicase activity specifically, DNA2 E675A, a mutant, nuclease-dead DNA2 variant was used. With the addition of DNA2 E675A in the presence of ATP and RPA, rapid DNA unwinding was observed through the lengthening of the DNA strand.
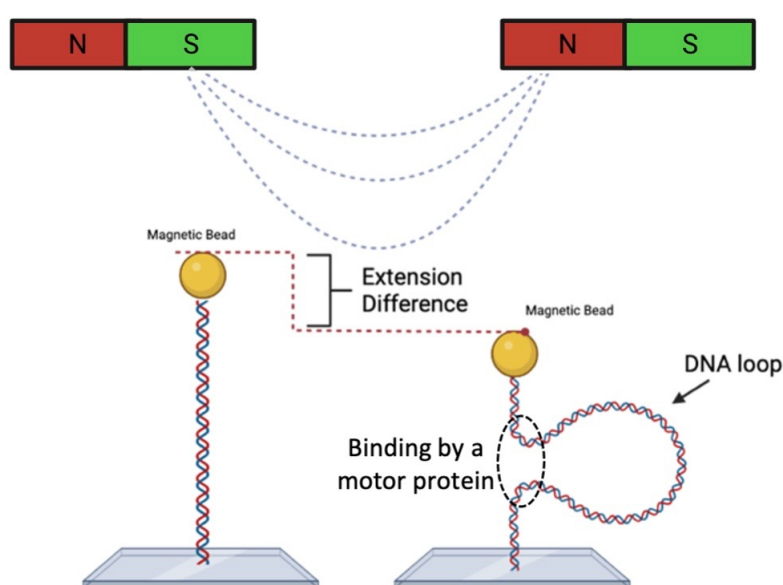
3.2. Study of DNA loops

Figure 9. Representation of DNA configurations in MTs, before and after loop extrusion. Loops occur when two different sites along the DNA molecules are brought together by a motor protein. This is followed by bending of DNA between the binding sites and a transient decrease in DNA extension.

In bacteria with circular chromosomes, recombination events often result in dimer formations that are harmful to the separation and segregation of newly replicated chromosomes following cell division [106]. To circumvent this issue, bacteria use site-specific recombinases that bind to *dif* sites [107]. XerC and XerD are the chromosomally encoded tyrosine recombinases found in *E. coli* [106]. Normally only one *dif* site is present on the *E. coli* chromosome but if unresolved dimers are present, two *dif* sites will be exhibited. The septal protein FtsK is responsible for controlling dimer resolution in cells and for ensuring that recombination occurs along the cell division septum precisely before division [106,108]. Additionally, FtsK acts as a motor protein that brings the *dif* sites in the correct placement to initiate recombinase binding [106]. FtsK has been studied extensively for its role in chromosomal preservation and antibiotic resistance, however the mechanism it employs to

translocate deleterious DNA segments is unclear. Preliminary findings suggested FtsK contributes to the extrusion of a DNA loop (Figure 9) [109], but real-time measurements and analysis are required to further these studies. The DNA loop occurs when a protein binds simultaneously to two different sites along the DNA, causing the DNA molecule between the two sites to bend [110].

The role of FtsK translocation to extrude loops is confirmed by single-molecule measurements. Saleh et al. [111] used MTs to directly monitor the translocation activity of FtsK *in vitro* (Figure 10). The extrusions of loops were manifested by a transient decrease in DNA extension. Using these results, they measured the length, duration, and velocity of each individual translocation event. They found that the direction of FtsK translocation can be reversed spontaneously, and the motor protein can travel both ways on the same DNA segment. Multiple theories have been proposed to explain the creation of the DNA loop, such as the presence of two motors translocating simultaneously, in which the DNA loop would be formed between the motors [112, 113]. Others hypothesize that multiple contact interactions may exist between a single motor and DNA, in which the DNA loop forms between the contact interactions [114].
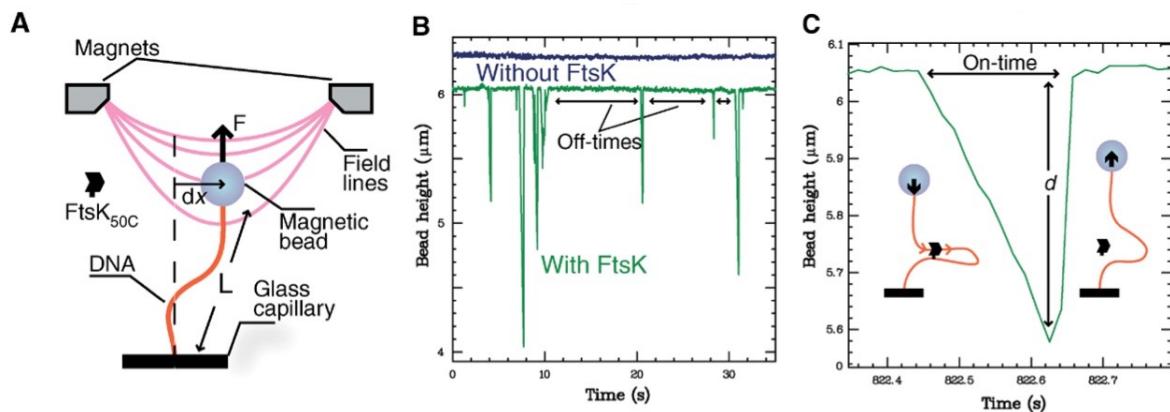

Figure 10. (A) A depiction of the experimental setup of MTs to study the loop extrusion by FtsK. The extension of the tether is monitored over time in the presence of FtsK and ATP. (B) Transient decreases in DNA extension show the creation of loops by FtsK. (C) Single extrusion event extracted from the data shown in B. The slope of the descent in DNA extension represents the translocation velocity of FtsK. Adapted from Saleh et al. [111].

3.3. Study of DNA elasticity

The bending of DNA molecules plays a critical role in gene expression, DNA replication, protein-DNA interactions, and DNA packaging. The way DNA is packaged within cells can affect how genes are expressed [115]. When DNA is tightly packed, it can be difficult for the transcription machinery to access specific genes, which can result in those genes being turned off. Bending DNA can expose certain genes to the cellular machinery present in the cell, making them more accessible for transcription and thus more readily expressed [116]. During replication, the double helix structure of DNA must be temporarily separated so that new strands can be synthesized. Bending of DNA facilitates the unwinding and separation of the DNA strands during replication [117]. Proteins that interact with DNA, such as transcription factors, often recognize specific DNA sequences and bind to them. Bending of DNA brings these protein-binding sites into close proximity. This makes it easier

for the proteins to bind and thereby increases transcription and amplifies expression of specific genes [116]. In eukaryotic cells, DNA is tightly packaged into chromatin, which is necessary for the compact storage of genetic material. Bending of DNA is essential for the formation of higher-order chromatin complexes, such as nucleosomes, which help to package DNA into a compact and organized structure [118].
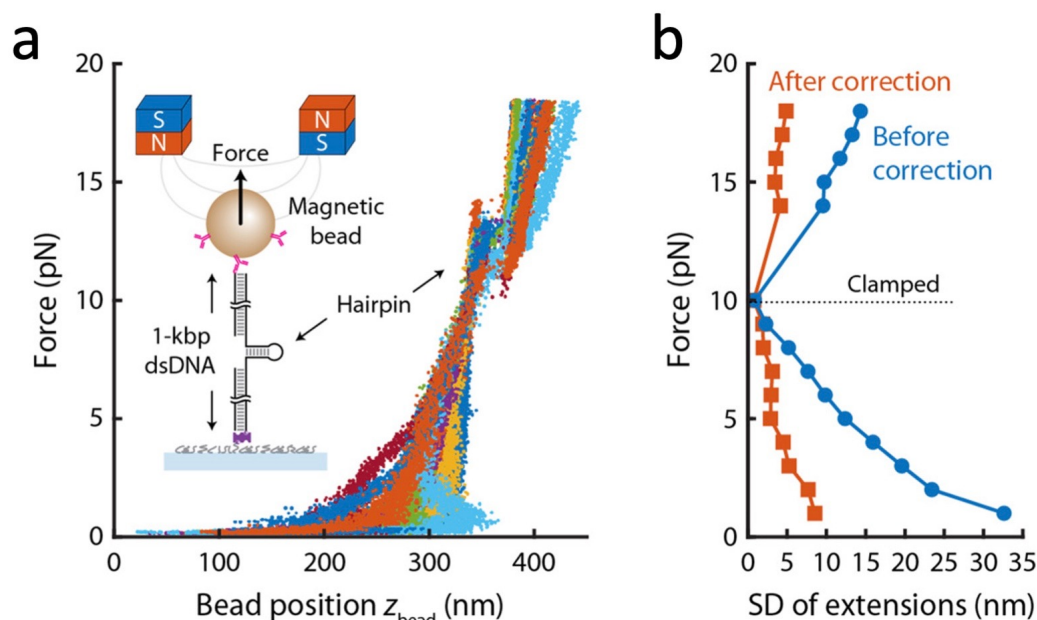

Figure 11. Force-extension curves from 16 short DNA tether constructs with 198 bps (67 nm) before extension correction. (b) Blue circles and red squares show the standard deviation of force-extension curves before and after extension correction, respectively. Dotted line shows 10 pN, where the extension was clamped for comparison. Adapted from Shon et al. [119].

In general, the number of admissible configurations of a DNA helix correlates with the number of added bp steps [120]. The length of dsDNA segments can be as short as 50 nm, equivalent to ~150 bps, making DNA bending energetically costly [119]. It is unclear how short dsDNA can bend and thereby undergo a thermodynamically unfavorable deformation. DNA elasticity has been analyzed using OTs, atomic force microscopy (AFM), and cryo-electron microscopy (cryo-EM) [121]. These methods of DNA studies on longer chains have confirmed the validity of WLC model for DNA elasticity, in which the DNA acts as a rod with a constant bending energy and length [122]. However, when dsDNA with ~150 bps or below are considered, experiments showed WLC does not hold true, as the DNA experienced increased flexibility [123]. OTs, AFM, and cryo-EM are often rendered inaccurate at smaller DNA lengths.

While MTs are useful in observing the force-extension relationship of short dsDNA through the diverse range of force levels it can deliver, several limitations exist. The most important drawback, perhaps, is that superparamagnetic beads have an anisotropy axis which, upon magnetization, will cause a variable, initial rotation of the bead [119, 124]. Thus, when subjected to an external magnetic field, the beads will orient themselves with the anisotropy axis, generating an erroneous torque, leading

to an underestimation in DNA extension [124]. Additionally, beads are often non uniform in size and in magnetic pigment content, which introduces bead-to-bead variability in the response to the magnetic field [125]. Shon et al. [119] tackled this problem using a DNA hairpin, in which an unpaired strand of DNA folds and anneals with another section of the same strand [126]. To obtain a scale factor of force on each magnetic bead, identical hairpins were placed in a DNA tether and the forces required to unzip the hairpins by each magnetic bead were measured [119]. With this application, they were able to create force-extension curves of short dsDNA close to the persistence length of ~150 bps and observe a great amount of sequence-dependent elasticity in real-time (Figure 11).

4. Modern advancements to MTs

The magnetic tweezing technology has advanced significantly since its debut. While the early generation of MTs were able to manipulate only one molecule at a time, the recent multiplexed MTs are capable of conducting parallel experiments on a large numbers of molecules in the same amount of time that a single-molecule measurement would require (Figure 12) [31, 127–129]. Studies show that multiplexed measurements are a faster way of obtaining data from magnetic tweezing for up to about 100 DNA-bead tethers [130]. When larger amounts of DNA-beads are studied, the process becomes cumbersome and the computational cost of real-time tracking of particles increases non-proportionally. However, implementing more efficient computational algorithms along with complementary metal-oxide-semiconductor (CMOS) cameras with high spatiotemporal resolutions [131–133] is expected to increase data acquisition rate for a large amounts of DNA-bead tethers at once [30, 127–130].
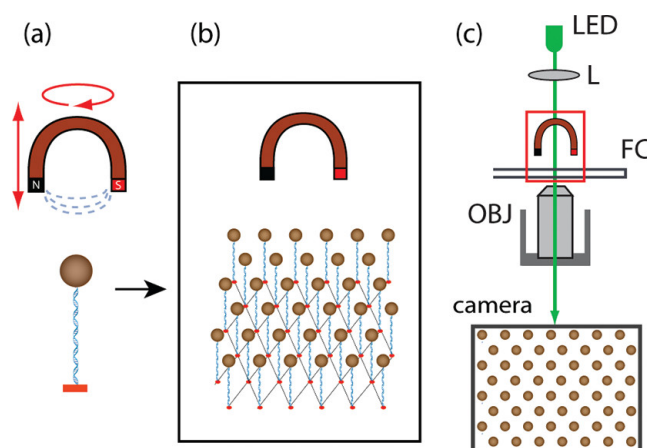

Figure 12. Parallelization increases data throughput by using multiplexed MTs. (a) Extension and rotation of single DNA tether using MTs. (b) Manipulation of a large number of DNA tethers to increase data throughput. (c) Schematic setting for the multiplexed MTs used by de Vlaminck et al. [31]. Adapted from de Vlaminck et al. [31] with permission. Copyright 2011 American Chemical Society.

Older generation of MTTs rely on one permanent magnet for both stretching force and rotational trapping potential. This leads to difficulties with decoupling force and torque generated by the tweezers [30, 134]. A solution to these problems is a new type of MTT that uses electromagnets and

permanent magnets, often referred to as electromagnetic torque tweezers (Figure 13). The use of electromagnets in conjunction with permanent magnets allows the technology to apply a wider range of stretching forces and independently control force and torsional stiffness traps. The latter is important because to make accurate torque measurements, the torsional stiffness trap should match the characteristic torques of the molecule being studied. [14, 135].
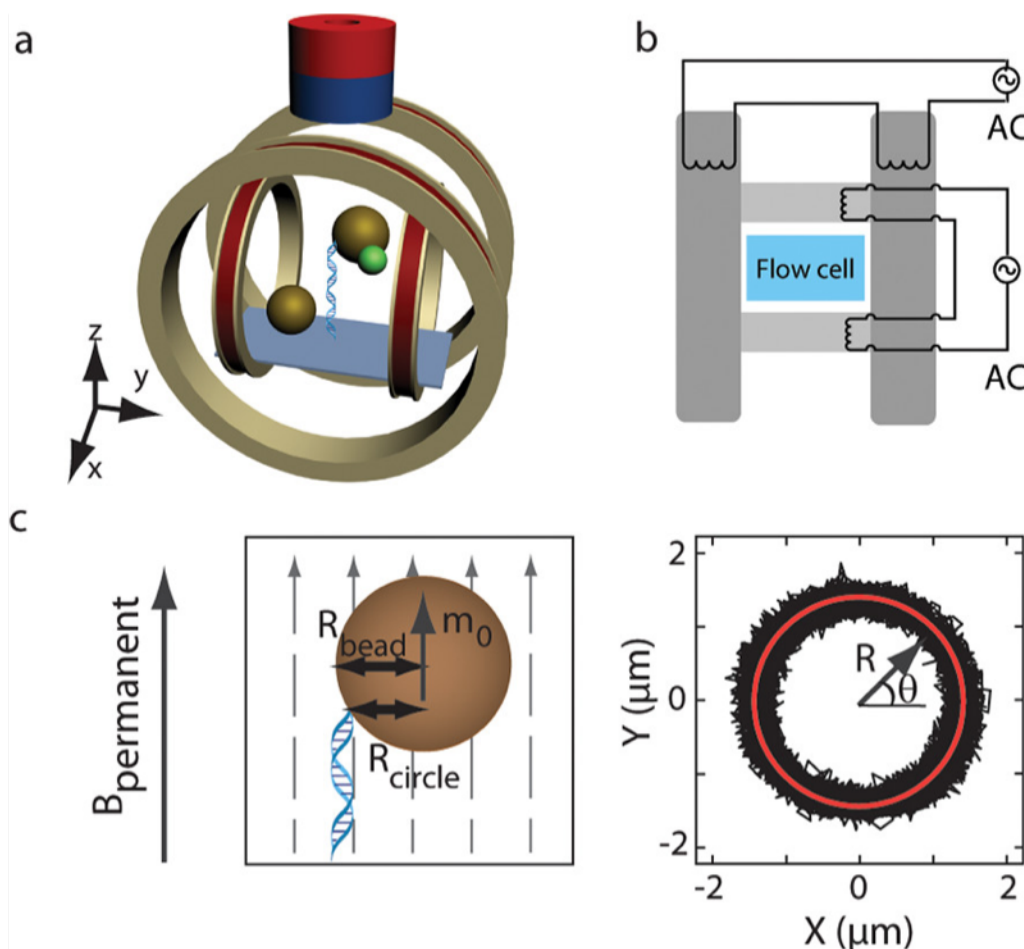

Figure 13. An illustration of the orientation of a DNA tether in the electromagnetic torque tweezers. (a) A DNA molecule is used to tether a paramagnetic bead to the surface of the flow cell. To correct for drift, another reference bead is fixed to the surface next to the tether. Four cylindrical coils generate a vertical force along the tether axis (z-axis), while the bead remains rotationally unconstrained. (b) The flow cell surrounded by the four cylindrical magnets (gray) and their electrical connections. (c) The bead is attached to the DNA somewhere between its equator and the poles. As m_0, the preferred magnetization axis of the bead, aligns parallel to the vertical field of permanent magnet $B_{permanent}$, its centroid follows an annulus as a result of thermal fluctuations. The stretching force on DNA can be found by measuring the fluctuations of radial position R. Adapted from de Janssen et al. [135] with permission. Copyright 2012 American Chemical Society.

MTs are usually composed of a single ferromagnetic core that is magnetized by winded

coils [136]. Application of single-pole MTs has multiple issues. They are capable of applying forces only in one direction. In addition, the strength of magnetic field in single-pole MTs decreases with the distance from the pole. It is therefore necessary to provide a high power output within a large working area in order to generate a sufficiently strong magnetic gradient. To overcome these challenges, multipole MTs were created to manipulate the superparamagnetic beads in multiple directions. The poles are symmetrically placed around the specimen to move the superparamagnetic beads in two or three dimensions [136, 137]. Multipole MTs are ideal devices to characterize the properties of different compartments of living cells [137]. Traditionally, OTs were used to manipulate the beads inside of living cells. They are unable to selectively operate in the intracellular environment as the high-intensity trapping laser could damage the specimens. The poles of multipole MTs can be positioned around a living cell to manipulate and navigate the position of a magnetic probe inside living cells or on their membranes [137]. Multipole MTs have been utilized to measure a wide variety of cell mechanical properties. This includes the viscoelastic properties of cell membrane, cytoskeleton, and nucleus [138]. Increasing the number of magnetic poles, however, yields larger degrees of freedom for magnetic force application. The small inertia and fast dynamics of magnetic probe may pose difficulties for position control, if the MTs are controlled in an open-loop manner [138]. The recent generations of multipole MTs rely on the feedback control law to stabilize and control the motion of a magnetic particle [139, 140].
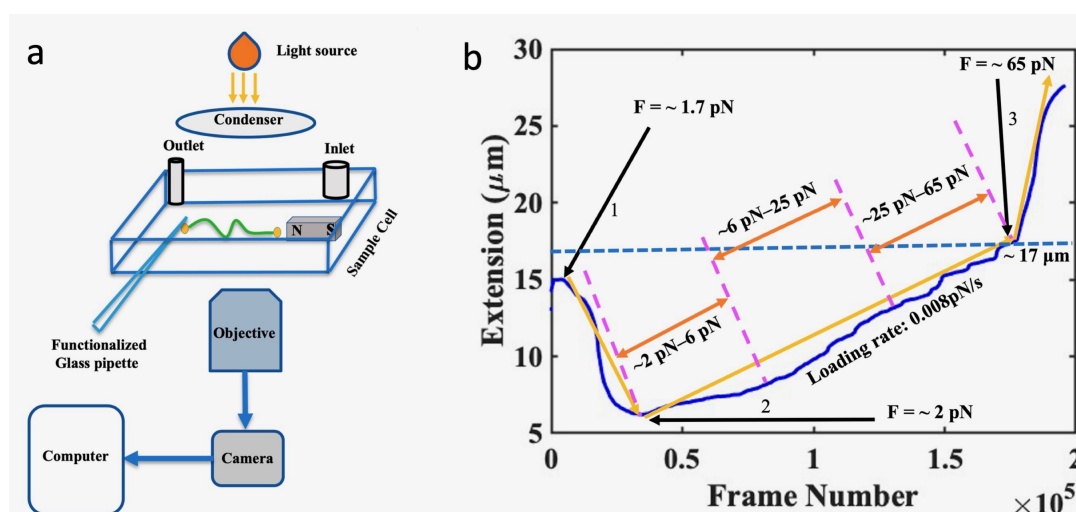

Figure 14. (a) MTs setting used by Gaire et al. [141] to demonstrate the force-dependent histone unbinding from DNA. (b) History of DNA extension before and after histone injection. Histones are initially bonded to a single DNA tether at a low extension (arrow 1). The force is slowly increased at a slow rate (from arrow 2). At a sufficiently large extension (arrow 3), the DNA tether ejects nearly all histone proteins. Adapted from Gaire et al. [141].

The modern application of magnetic tweezers continues to illuminate different aspects of DNA-proteins interactions. An important example is the effect of histone on chromosomal DNA. Histones play a critical role in organizing and packing DNA into a compact structure called chromatin [142]. By wrapping around DNA, histones reduce the overall volume of the DNA molecule and allow for

more efficient storage of genetic information within the cell nucleus. In addition, this regulation of chromatin structure by histone allows cells to control gene expression, as it can determine which parts of the DNA are accessible to the cellular machinery responsible for gene expression. MTs have been used to demonstrate the role of histone in DNA compaction and to understand how changes in histone modifications can regulate the mechanical properties of chromatin fibers and gene expression [141, 143]. The experimental setting for the horizontal MTs used by Gaire et al. [141] is shown in Figure 14. Histone proteins were injected and interacted with DNA that was stretched with a small force of 1 pN. The tether was stretched by this force but it did not impede the spontaneous assembly of histones onto the DNA. The histone-DNA tether was then subjected to higher forces to begin dissociating histones. The onset of dissociation was detected by a jump in tether extension (Figure 14(b)). Understanding the underlying physics of competitive histone binding to DNA in the presence of transcription factors is of great importance in biophysics and biochemistry. A number of models are proposed to explain the role of histone in chromatin compaction and particularly the synergistic interactions between the histone tails, linker histones, and ions [144, 145]. It is known that the intensity of interactions between the nucleosome core particles depends on the helical pattern of charges on the surface of DNA, which in turn affects the electrostatic interactions of nucleosome core particles in chromatin [146, 147].

MTs have recently been used in conjunction with fluorescence spectroscopy to efficiently measure structural changes within nucleic acids under low stretching forces [148]. The use of MTs alone requires relatively long flexible DNA strands. While these long strands facilitate micromanipulation, they also introduce noise into the system, reducing the spatial resolution of the measurements. In order to increase the spatial resolution, high stretching forces are applied to subdue the noise generated by DNA. This can be achieved by combining force-fluorescence spectroscopy with MTs to measure the conformational changes within individual molecules. The integration of two systems is relatively simple and would allow many laboratories to have access to this technology [148]. With these two systems working in conjunction, this technology can simultaneously observe and manipulate nanoscale structural transitions over a wide range of forces. This technique has been used in experiments to help study DNA molecules under torque. One such experiment detected B-to-Z DNA transition while under torsion and tension. This transition occurred under minimal negative superhelicity and low tension. Without the use of MTs and force-fluorescence spectroscopy, this transition would not have been able to be measured [148].

5. Conclusions

Over the last few decades, MTs have emerged as an innovative tool for studying DNA and DNA-protein interactions at the molecular level. Due to their versatility and ease of operation, MTs offer multiple advantages over other tools used to study DNA. Different types of MTs can be used to apply forces and torque to study DNA elasticity and understand the functions of proteins that characterize DNA transcription, repair, and replication. In particular, the mechanisms and functions of nucleases, topoisomerases, and helicases have been extensively advanced through MT technology, as DNA unwinding can be measured through DNA extension. Recent advancements, such as multiplexed measurements, have improved the speed and efficiency of spectroscopy by allowing for more than one sample to be studied at a time [127, 149]. Electromagnetic torque tweezers have enhanced the performance of MTTs by allowing the torsional stiffness trap and force to be controlled

separately. Micro-MTs allow for multiple MTs to be placed within a small distance to study the mechanical properties of cell compartments. It has been almost 70 years since Crick and Hughes [2] pioneered the use of magnetic forces to study biological systems, but this exciting field continues to grow and expand to new developments in biophysics and life sciences.

Use of AI tools declaration

The authors declare they have not used Artificial Intelligence (AI) tools in the creation of this article.

Acknowledgments

Conflict of interest

The authors declare that there are no conflict of interests.

References

1. Bustamante CJ, Chemla YR, Liu S, et al. (2021) Optical tweezers in single-molecule biophysics. *Nat Rev Method Prime* 1: 25. `https://doi.org/10.1038/s43586-021-00021-6`

2. Crick FHC, Hughes AFW (1950) The physical properties of cytoplasm: A study by means of the magnetic particle method Part I. Experimental. *Exp Cell Res* 1: 37–80. `https://doi.org/10.1016/0014-4827(50)90048-6`

3. Valberg PA, Albertini DF (1985) Cytoplasmic motions, rheology, and structure probed by a novel magnetic particle method. *J Cell Biol* 101: 130–140. `https://DOI:10.1083/jcb.101.1.130`

4. Shi Y, Sivarajan S, Crocker JC, et al. (2022) Measuring cytoskeletal mechanical fluctuations and rheology with active micropost arrays. *Curr Protoc* 2: e433. `https://doi.org/10.1002/cpz1.433`

5. Lipfert J, Lee M, Ordu O, et al. (2014) Magnetic tweezers for the measurement of twist and torque. *J Vis Exp* 87: e51503. `https://doi.org/10.3791/51503`

6. Smith SB, Finzi L, Bustamante C (1992) Direct mechanical measurements of the elasticity of single DNA molecules by using magnetic beads. *Science* 258: 1122–1126. `https://doi.org/10.1126/science.1439819`

7. Bouchiat C, Wang MD, Allemand J, et al. (1999) Estimating the persistence length of a worm-like chain molecule from force-extension measurements. *Biophys J* 76:409–413. `https://doi.org/10.1016/s0006-3495(99)77207-3`

8. Strick TR, Dessinges MN, Charvin G, et al. (2003) Stretching of macromolecules and proteins. *Rep Prog Phys* 66: 1–45. `https://DOI10.1088/0034-4885/66/1/201`

9. Gollnick B (2015) *Optical and magnetic tweezers for applications in single-molecule biophysics and nanotechnology*. Doctoral Thesis, Universidad Autónoma de Madrid. `https://produccioncientifica.ucm.es/documentos/5d39994f299952068444143c`

10. Strick TR, Allemand JF, Bensimon D, et al. (1996) The elasticity of a single supercoiled DNA molecule. *Science* 271: 1835–1837. `https://doi.org/10.1126/science.271.5257.1835`

11. Bustamante C, Bryant Z, Smith SB (2003) Ten years of tension: single-molecule DNA mechanics. *Nature* 421: 423–427. `https://doi.org/10.1038/nature01405`

12. Vilfan ID, Lipfert J, Koster DA, et al. (2009) Magnetic tweezers for single-molecule experiments, *Handbook of Single-Molecule Biophysics*, 371–395. `https://doi.org/10.1007/978-0-387-76497-9`

13. Seol Y, Neuman KC (2011) Magnetic tweezers for single-molecule manipulation, *Single Molecule Analysis: Methods and Protocols*, 265–293. `https://doi.org/10.1007/978-1-4939-7271-5`

14. Kilinc D, Lee GU (2014) Advances in magnetic tweezers for single molecule and cell biophysics. *Integr Biol* 6: 27–34. `https://doi.org/10.1039/c3ib40185e`

15. Dulin D, Berghuis BA, Depken M (2015) Untangling reaction pathways through modern approaches to high-throughput single-molecule force-spectroscopy experiments. *Curr Opin Struc Biol* 34: 116–122. `https://doi.org/10.1016/j.sbi.2015.08.007`

16. Sarkar R, Rybenkov VV (2016) A guide to magnetic tweezers and their applications. *Front Phys* 4: 48. urlhttps://doi.org/ARTN4810.3389/fphy.2016.00048

17. Berghuis BA, Köber M, van Laar T, et al. (2016) High-throughput, high-force probing of DNA-protein interactions with magnetic tweezers. *Methods* 105: 90–98. `https://doi.org/10.1016/j.ymeth.2016.03.025`

18. Mandal SS (2020) Force spectroscopy on single molecules of life. *ACS Omega* 5: 11271–11278. `https://doi.org/10.1021/acsomega.0c00814`

19. Zacchia, NA, Valentine MT(2015) Design and optimization of arrays of neodymium iron boron-based magnets for magnetic tweezers applications. *Rev Sci Instrum* 86: 053704. `https://doi.org/Artn05370410.1063/1.4921553`

20. Jiang C, Lionberger TA, Wiener DM, et al. (2015) Electromagnetic tweezers with independent force and torque control. *Rev Sci Ins* 87: 084304. `https://doi.org/DOI10.1016/j.bpj.2014.11.1946`

21. Humphries DE, Hong S, Pollard MJ, et al. (2009) Hybrid magnet devices for molecule manipulation and small scale high gradient-field applications, Patent. Lawrence Berkeley National Lab, Berkeley, CA.

22. Fu CM, Han CM, Cheng CW, et al. (2012) Bio-mechanical properties of human renal cancer cells probed by magneto-optical tweezers. *Sensors, 2012 IEEE* 111–114. `https://doi.org/10.1109/ICSENS.2012.6411557`

23. Strick TR, Allemand JF, Croquette V, et al. (1998) Physical approaches to the study of DNA. *J Stat Phys* 93: 647–672. `https://doi.org/DOI10.1023/B:JOSS.0000033247.51868.be`

24. Kriegel F, Ermann N, Forbes R, et al. (2017) Probing the salt dependence of the torsional stiffness of DNA by multiplexed magnetic torque tweezers. *Nucleic Acids Res* 45: 5920–5929. `https://doi.org/10.1093/nar/gkx280`

25. Mosconi F, Allemand JF, Croquette V (2011) Soft magnetic tweezers: A proof of principle. *Rev Sci Instrum* 82: 3. `https://doi.org/Artn03430210.1063/1.3531959`

26. Lipfert J, van Oene MM, Lee M, et al. (2015) Torque spectroscopy for the study of rotary motion in biological systems. *Chem Rev* 115: 1449–1474. `https://doi.org/10.1021/cr500119k`

27. Lipfert J, Wiggin M, Kerssemakers JWJ, et al. (2011) Freely orbiting magnetic tweezers to directly monitor changes in the twist of nucleic acids. *Nat Commun* 2: 439. `https://doi.org/ARTN43910.1038/ncomms1450`

28. Bryant Z, Oberstrass, FC, Basu A (2012) Recent developments in single-molecule DNA mechanics. *Curr Opin Struct Biol* 22: 304–312. `https://doi.org/10.1016/j.sbi.2012.04.007`

29. Cox MM (2000) Recombinational DNA repair in bacteria and the RecA protein. *Prog Nucleic Acid Res Mol Biol* 63: 311–366. `https://doi.org/Doi10.1016/S0079-6603(08)60726-6`

30. Lipfert J, Kerssemakers JWJ, Jager T, et al. (2010) Magnetic torque tweezers: measuring torsional stiffness in DNA and RecA-DNA filaments. *Nat Methods* 7: 977–980. `https://doi.org/10.1038/Nmeth.1520`

31. De Vlaminck I, Henighan T, van Loenhout MTJ, et al. (2011) Highly parallel magnetic tweezers by targeted DNA tethering. *Nano Lett* 11: 5489–5493. `https://doi.org/10.1021/nl203299e`

32. Lipfert J, Koster DA, Vilfan ID, et al. (2009) Single-molecule magnetic tweezers studies of type IB topoisomerases, *DNA Topoisomerases: Methods and Protocols*, 71–89. `https://doi.org/10.1007/978-1-60761-340-4`

33. Yu ZB, Dulin D, Cnossen J, et al. (2014) A force calibration standard for magnetic tweezers. *Rev Sci Instrum* 85: 12. `https://doi.org/Artn12311410.1063/1.4904148`

34. Neuman KC, Lionnet T, Allemand JF (2007) Single-molecule micromanipulation techniques. *Annu Rev Mater Res* 37: 33–67. `https://doi.org/10.1146/annurev.matsci.37.052506.084336`

35. Lipfert J, Hao XM, Dekker NH (2009) Quantitative modeling and optimization of magnetic tweezers. *Biophys J* 96: 5040–5049. `https://doi.org/10.1016/j.bpj.2009.03.055`

36. Wong WP, Halvorsen K (2006) The effect of integration time on fluctuation measurements: calibrating an optical trap in the presence of motion blur. *Opt Express* 14: 12517–12531. `https://doi.org/Doi10.1364/Oe.14.012517`

37. Savin T, Doyle PS (2005) Static and dynamic errors in particle tracking microrheology. *Biophys J* 88: 623–638. `https://doi.org/10.1529/biophysj.104.042457`

38. Velthuis AJWT, Kerssemakers JWJ, Lipfert J, et al. (2010) Quantitative guidelines for force calibration through spectral analysis of magnetic tweezers data. *Biophys J* 99: 1292–1302. `https://doi.org/10.1016/j.bpj.2010.06.008`

39. Bell SP, Dutta A (2002) DNA replication in eukaryotic cells. *Annu Rev Biochem* 71: 333–374. `https://doi.org/10.1146/annurev.biochem.71.110601.135425`

40. Friedberg EC, Walker GC, Siede W, et al. (2005) *DNA Repair and Mutagenesis*, American Society for Microbiology Press.

41. Friedberg EC, Aguilera A, Gellert M, et al. (2006) DNA repair: from molecular mechanism to human disease. *DNA Repair* 5: 986–996. `https://doi.org/10.1016/j.dnarep.2006.05.005`

42. Matson SW, Bean DW, George JW (1994) DNA helicases–Enzymes with essential roles in all aspects of DNA metabolism. *Bioessays* 16: 13–22. `https://doi.org/DOI10.1002/bies.950160103`

43. Pray L (2008) Major molecular events of DNA replication. *Nat Educ* 1: 99.

44. Friedberg EC (2003) DNA damage and repair. *Nature* 421: 436–440. `https://doi.org/10.1038/nature01408`

45. Mota MBS, Carvalho MA, Monteiro ANA, et al. (2019) DNA damage response and repair in perspective: Aedes aegypti, drosophila melanogaster and homo sapiens. *Parasite Vector* 12: 1–20. `https://doi.org/ARTN53310.1186/s13071-019-3792-1`

46. Krokan HE, Bjørås M (2013) Base excision repair. *CSH Perspect Biol* 5: a012583. `https://doi.org/10.1101/cshperspect.a012583`

47. Li X, Heyer WD (2008) Homologous recombination in DNA repair and DNA damage tolerance. *Cell Res* 18: 99–113. `https://doi.org/10.1038/cr.2008.1`

48. de Laat WL, Jaspers NGJ, Hoeijmakers JHJ (1999) Molecular mechanism of nucleotide excision repair. *Gene Dev* 13: 768–785. `https://doi.org/DOI10.1101/gad.13.7.768`

49. Kunkel TA, Erie DA (2005) DNA mismatch repair. *Annu Rev Genet* 74: 681–710. `https://doi.org/10.1146/annurev-genet-112414-054722`

50. Weterings E, Chen DJ (2008) The endless tale of non-homologous end-joining. *Cell Res* 18: 114–124. `https://doi.org/10.1038/cr.2008.3`

51. Koster DA, Crut A, Shuman S, et al. (2010) Cellular strategies for regulating DNA supercoiling: a single-molecule perspective. *Cell* 142: 519–530. `https://doi.org/10.1016/j.cell.2010.08.001`

52. Ma J, Wang MD (2016) DNA supercoiling during transcription. *Biophys Rev* 8: 75–87. `https://doi.org/10.1007/s12551-016-0215-9`

53. Zlatanova J, Leuba SH (2003) Magnetic tweezers: a sensitive tool to study DNA and chromatin at the single-molecule level. *Biochem Cell Biol* 81: 151–159. `https://doi.org/10.1139/o03-048`

54. Dekker NH, Rybenkov VV, Duguet M, et al. (2002) The mechanism of type IA topoisomerases. *Proceedings of the National Academy of Sciences of the United States of America* 99: 12126-12131. `https://doi.org/10.1073/pnas.132378799`

55. Strick TR, Allemand JF, Bensimon D, et al. (1998) Behavior of supercoiled DNA. *Biophys J* 74: 2016–2028. `https://doi.org/Doi10.1016/S0006-3495(98)77908-1`

56. Allemand JF, Bensimon D, Lavery R, et al. (1998) Stretched and overwound DNA forms a Pauling-like structure with exposed bases. *Proceedings of the National Academy of Sciences of the United States of America* 95: 14152-14157. `https://doi.org/DOI10.1073/pnas.95.24.14152`

57. Dessinges MN, Maier B, Zhang Y, et al. (2002) Stretching single stranded DNA, a model polyelectrolyte. *Phys Rev Lett* 89: 248102. `https://doi.org/ARTN24810210.1103/PhysRevLett.89.248102`

58. Seol Y, Gentry AC, Osheroff N, et al. (2013) Chiral discrimination and writhe-dependent relaxation mechanism of human topoisomerase IIalpha. *J Biol Chem* 288: 13695–13703. `https://doi.org/10.1074/jbc.M112.444745`

59. Wang JC (1998) Moving one DNA double helix through another by a type II DNA topoisomerase: the story of a simple molecular machine. *Q Rev Biophys* 31: 107–144. `https://doi.org/10.1017/s0033583598003424`

60. Wang JC (2002) Cellular roles of DNA topoisomerases: a molecular perspective. *Nat Rev Mol Cell Biol* 3: 430–440. `https://doi.org/10.1038/nrm831`

61. Travers A, Muskhelishvili G (2005) DNA supercoiling–a global transcriptional regulator for enterobacterial growth? *Nat Rev Microbiol* 3: 157–169. `https://doi.org/10.1038/nrmicro1088`

62. Stewart L, Redinbo MR, Qiu XY, et al. (1998) A model for the mechanism of human topoisomerase I. *Science* 279: 1534–1541. `https://doi.org/DOI10.1126/science.279.5356.1534`

63. Forterre P, Gadelle D (2009) Phylogenomics of DNA topoisomerases: their origin and putative roles in the emergence of modern organisms. *Nucleic Acids Res* 37: 679–692. `https://doi.org/10.1093/nar/gkp032`

64. Corbett KD, Berger JM (2004) Structure, molecular mechanisms, and evolutionary relationships in DNA topoisomerases. *Annu Rev Biophys Biomol Struct* 33: 95–118. `https://doi.org/DOI10.1146/annurev.biophys.33.110502.140357`

65. Charvin G, Strick TR, Bensimon D, et al. (2005) Tracking topoisomerase activity at the single-molecule level. *Annu Rev Biophys Biomol Struct* 34: 201–219. `https://doi.org/DOI10.1146/annurev.biophys.34.040204.144433`

66. Neuman KC (2010) Single-molecule measurements of DNA topology and topoisomerases. *J Biol Chem* 285: 18967–18971. `https://doi.org/10.1074/jbc.R109.092437`

67. Seol Y, Neuman KC (2011) Single-molecule measurements of topoisomerase activity with magnetic tweezers. *Single Mol Enzymol: Method Protoc* 229–241. `https://doi.org/10.1007/978-1-61779-261-8`

68. Gunn KH, Marko JF, Mondragón A (2018) Single-molecule magnetic tweezer analysis of topoisomerases. *DNA Topoisomerases* 139–152. `https://doi.org/10.1007/978-1-4939-7459-7`

69. Spakman D, Bakx JAM, Biebricher AS, et al. (2021) Unraveling the mechanisms of type 1A topoisomerases using single-molecule approaches. *Nucleic Acids Res* 49: 5470–5492. `https://doi.org/10.1093/nar/gkab239`

70. Koster DA, Croquette V, Dekker C, et al. (2005) Friction and torque govern the relaxation of DNA supercoils by eukaryotic topoisomerase IB. *Nature* 434: 671–674. `https://doi.org/10.1038/nature03395`

71. Strick TR, Croquette V, Bensimon D (2000) Single-molecule analysis of DNA uncoiling by a type II topoisomerase. *Nature* 404: 901–904. `https://doi.org/Doi10.1038/35009144`

72. Neuman KC, Charvin G, Bensimon D (2009) Mechanisms of chiral discrimination by topoisomerase IV. *Proceedings of the National Academy of Sciences of the United States of America* 106: 6986–6991. `https://doi.org/10.1073/pnas.0900574106`

73. Crisona NJ, Strick TR, Bensimon D, et al. (2000) Preferential relaxation of positively supercoiled DNA by E-coli topoisomerase IV in single-molecule and ensemble measurements. *Gene Dev* 14: 2881–2892. `https://doi.org/DOI10.1101/gad.838900`

74. Taneja B, Schnurr B, Slesarev A, et al. (2007) Topoisomerase V relaxes supercoiled DNA by a constrained swiveling mechanism. Proceedings of the *National Academy of Sciences of the United States of America* 104: 14670–14675. `https://doi.org/10.1073/pnas.0701989104`

75. Seol Y, Zhang HL, Pommier Y, et al. (2012) A kinetic clutch governs religation by type IB topoisomerases and determines camptothecin sensitivity. *Proceedings of the National Academy of Sciences of the United States of America* 109: 16125–16130. `https://doi.org/10.1073/pnas.1206480109`

76. McKie SJ, Desai PR, Seol Y, et al. (2022) Topoisomerase VI is a chirally-selective, preferential DNA decatenase. *Elife* 11: e67021. `https://doi.org/ARTNe6702110.7554/eLife.67021`

77. Levine C, Hiasa H, Marians KJ (1998) DNA gyrase and topoisomerase IV: Biochemical activities, physiological roles during chromosome replication, and drug sensitivities. *BBA-Gene Struct Expr* 1400: 29–43. `https://doi.org/Doi10.1016/S0167-4781(98)00126-2`

78. Charvin G, Bensimon D, Croquette V (2003) Single-molecule study of DNA unlinking by eukaryotic and prokaryotic type-II topoisomerases. *Proceedings of the National Academy of Sciences of the United States of America* 100: 9820–9825. `https://doi.org/10.1073/pnas.1631550100`

79. Tanaka F, Takahashi H (1985) Elastic theory of supercoiled DNA. *J Chem Phys* 83: 6017–6026. `https://doi.org/Doi10.1063/1.449637`

80. Thompson JMT, van der Heijden GHM, Neukirch S (2002) Supercoiling of DNA plasmids: mechanics of the generalized ply. *Proceedings of the Royal Society a-Mathematical Physical and Engineering Sciences* 458: 959–985. `https://doi.org/10.1098/rspa.2001.0901`

81. Marko JF (1997) Supercoiled and braided DNA under tension. *Phys Rev E* 55: 1758–1772. `https://doi.org/DOI10.1103/PhysRevE.55.1758`

82. Rybenkov VV, Cozzarelli NR, Vologodskii AV (1993) Probability of DNA knotting and the effective diameter of the DNA double helix. *Proceedings of the National Academy of Sciences of the United States of America* 90: 5307–5311. `https://doi.org/DOI10.1073/pnas.90.11.5307`

83. Timsit Y, Várnai P (2010) Helical chirality: a Link between local interactions and global topology in DNA. *PLoS One* 5: e9326. `https://doi.org/ARTNe932610.1371/journal.pone.0009326`

84. Vologodskii A (2009) Theoretical models of DNA topology simplification by type IIA DNA topoisomerases. *Nucleic Acids Res* 37: 3125–3133. `https://doi.org/10.1093/nar/gkp250`

85. Liu ZR, Deibler RW, Chan HS, et al. (2009) The why and how of DNA unlinking. *Nucleic Acids Res* 37: 661–671. `https://doi.org/10.1093/nar/gkp041`

86. Dong KC, Berger JM (2007) Structural basis for gate-DNA recognition and bending by type IIA topoisomerases. *Nature* 450: 1201–1204. `https://doi.org/10.1038/nature06396`

87. Yan J, Magnasco MO, Marko JF (1999) A kinetic proofreading mechanism for disentanglement of DNA by topoisomerases. *Nature* 401: 932–935. `https://doi.org/Doi10.1038/44872`

88. Trigueros S, Salceda J, Bermúdez I, et al. (2004) Asymmetric removal of supercoils suggests how topoisomerase II simplifies DNA topology. *J Mol Biol* 335: 723-–731. `https://doi.org/10.1016/j.jmb.2003.11.011`

89. Liu Z, Mann JK, Zechiedrich EL, et al. (2006) Topological information embodied in local juxtaposition geometry provides a statistical mechanical basis for unknotting by type-2 DNA topoisomerases. *J Mol Biol* 361: 268-–285. `https://doi.org/10.1016/j.jmb.2006.06.005`

90. Zechiedrich EL, Osheroff N (1990) Eukaryotic topoisomerases recognize nucleic acid topology by preferentially interacting with DNA crossovers. *EMBO J* 9: 4555-–4562. `https://doi.org/10.1002/j.1460-2075.1990.tb07908.x`

91. Cherstvy AG (2009) Probing DNA-DNA electrostatic friction in tight superhelical DNA plies. *J Phys Chem B* 113: 5350–5355. `https://doi.org/10.1021/jp810473m`

92. Randall GL, Pettitt BM, Buck GR, et al. (2006) Electrostatics of DNA-DNA juxtapositions: consequences for type II topoisomerase function. *J Phys Condens Matter* 18: S173–S185. `https://doi.org/10.1088/0953-8984/18/14/S03`

93. Kornyshev AA, Leikin S, Malinin SV (2002) Chiral electrostatic interaction and cholesteric liquid crystals of DNA. *Eur Phys J E* 7: 83–93. `https://doi.org/10.1140/epje/i200101159`

94. Knoll A, Puchta H (2011) The role of DNA helicases and their interaction partners in genome stability and meiotic recombination in plants. *J Exp Bot* 62: 1565–1579. `https://doi.org/21081662`

95. Yodh JG, Schlierf M, Ha T (2010) Insight into helicase mechanism and function revealed through single-molecule approaches. *Q Rev Biophys* 43: 185–217. `https://doi.org/10.1017/S0033583510000107`

96. Hodeib S, Raj S, Manosas M, et al. (2016) Single molecule studies of helicases with magnetic tweezers. *Methods* 105: 3–15. `https://doi.org/10.1016/j.ymeth.2016.06.019`

97. Nandakumar D, Patel SS (2016) Methods to study the coupling between replicative helicase and leading-strand DNA polymerase at the replication fork. *Methods* 108: 65–78. `https://doi.org/10.1016/j.ymeth.2016.05.003`

98. Spies M (2012) *DNA helicases and DNA motor proteins* Springer Science and Business Media. `https://doi.org/10.1007/978-1-4614-5037-5`

99. Dessinges MN, Lionnet T, Xi XG, et al. (2004) Single-molecule assay reveals strand switching and enhanced processivity of UvrD. *Proceedings of the National Academy of Sciences of the United States of America* 101: 6439–6444. `https://doi.org/10.1073/pnas.0306713101`

100. Lionnet T, Spiering MM, Benkovic SJ, et al. (2007) Real-time observation of bacteriophage T4 gp41 helicase reveals an unwinding mechanism. *Proceedings of the National Academy of Sciences of the United States of America* 104: 19790–19795. `https://doi.org/10.1073/pnas.0709793104`

101. Ramanathan SP, van Aelst K, Sears A, et al. (2009) Type III restriction enzymes communicate in 1D without looping between their target sites. *Proceedings of the National Academy of Sciences of the United States of America* 106: 1748–1753. `https://doi.org/10.1073/pnas.0807193106`

102. Sun B, Wei KJ, Zhang B, et al. (2008) Impediment of E. coli UvrD by DNA-destabilizing force reveals a strained-inchworm mechanism of DNA unwinding. *EMBO J* 27: 3279–3287. `https://doi.org/10.1038/emboj.2008.240`

103. Nishino T, Morikawa K (2002) Structure and function of nucleases in DNA repair: shape, grip and blade of the DNA scissors. *Oncogene* 21: 9022–9032. `https://doi.org/10.1038/sj.onc.1206135`

104. Carrasco C, Gilhooly NS, Dillingham MS, et al. (2013) On the mechanism of recombination hotspot scanning during double-stranded DNA break resection. *Proceedings of the National Academy of Sciences of the United States of America* 110: E2562–E2571. `https://doi.org/10.1073/pnas.1303035110`

105. Levikova M, Klaue D, Seidel R, et al. (2013) Nuclease activity of Saccharomyces cerevisiae DNA2 inhibits its potent DNA helicase activity. *Proceedings of the National Academy of Sciences of the United States of America* 110: E1992–E2001. `https://doi.org/10.1073/pnas.1300390110`

106. Castillo F, Benmohamed A, Szatmari G (2017) Xer site specific recombination: Double and single recombinase systems. *Front MicrobioL* 8: 453. `https://doi.org/10.3389/fmicb.2017.00453`

107. Manosas M, Meglio A, Spiering MM, ET AL. (2010). Magnetic tweezers for the study of DNA tracking motors. *Method Enzymol* 475: 297–320. `https://doi.org/10.1016/S0076-6879(10)75013-8`

108. Cameranesi MM, Morán-Barrio J, Limansky AS, et al. (2018) Site-specific recombination at XerC/D sites mediates the formation and resolution of plasmid co-integrates carrying a blaOXA-58- and tnaphA6-resistance module in acinetobacter baumannii. *Front Microbiol* 9: 66. `https://doi.org/10.3389/fmicb.2018.00066`

109. Aussel L, Barre FX, Aroyo M, et al. (2002) FtsK Is a DNA motor protein that activates chromosome dimer resolution by switching the catalytic state of the XerC and XerD recombinases. *Cell* 108:195–205. `https://doi.org/10.1016/s0092-8674(02)00624-4`

110. Allemand JF, Bensimon D, Charvin G, et al. (2007) Studies of DNA-protein interactions at the single molecule level with magnetic tweezers. *Controlled Nanoscale Motion: Nobel Symposium 131*, 123–140. `https://doi.org/10.1007/3-540-49522-3`

111. Saleh OA, Pérals C, Barre FX, et al. (2004) Fast, DNA-sequence independent translocation by FtsK in a single-molecule experiment. *EMBO J* 23: 2430–2439. `https://doi.org/10.1038/sj.emboj.7600242`

112. Crozat E, Grainge I (2010) FtsK DNA translocase: the fast motor that knows where it is going. *Chembiochem : Eur J Chem Biol* 11: 2232–2243. `https://doi.org/10.1002/cbic.201000347`

113. Ip SC, Bregu M, Barre FX, et al. (2003) Decatenation of DNA circles by FtsK-dependent Xer site-specific recombination. *EMBO J* 22: 6399–6407. `https://doi.org/10.1093/emboj/cdg589`

114. Pease PJ, Levy O, Cost GJ, et al. (2005) Sequence-directed DNA translocation by purified FtsK. *Science* 307: 586–590. `https://doi.org/10.1126/science.1104885`

115. Annunziato A (2008) DNA packaging: Nucleosomes and chromatin. *Nat Educ* 1: 26

116. van der Vliet PC, Verrijzer CP (1993) Bending of DNA by transcription factors. *BioEssays* 15: 25–32. `https://doi.org/10.1002/bies.950150105`

117. Grimwade JE, Leonard AC (2021) Blocking, bending, and binding: Regulation of initiation of chromosome replication during the escherichia coli cell cycle by transcriptional modulators that interact with origin DNA. *Front Microbiol* 12: 732270. `https://doi.org/10.3389/fmicb.2021.732270`

118. Garcia HG, Grayson P, Han L, et al. (2007) Biological consequences of tightly bent DNA: the other life of a macromolecular celebrity. *Biopolymers* 85: 115–130. `https://doi.org/10.1002/bip.20627`

119. Shon MJ, Rah SH, Yoon TY (2019) Submicrometer elasticity of double-stranded DNA revealed by precision force-extension measurements with magnetic tweezers. *Sci Adv* 5: eaav1697. `https://doi.org/10.1126/sciadv.aav1697`

120. Zheng G, Czapla L, Srinivasan AR, et al. (2010) How stiff is DNA? *Phys Chem Chem Phys* 12: 1399–1406. `https://doi.org/10.1039/b916183j`

121. Peters JP, Maher LJ (2010) DNA curvature and flexibility in vitro and in vivo. *Q Rev Biophys* 43: 23–63. `https://doi.org/10.1017/S0033583510000077`

122. Butt HJ, Cappella B, Kappl M (2005) Force measurements with the atomic force microscope: Technique, interpretation and applications. *Surf Sci Rep* 59: 1–152. `https://doi.org/10.1016/j.surfrep.2005.08.003`

123. Cloutier TE, Widom J (2004) Spontaneous sharp bending of double-stranded DNA. *Mol Cell* 14: 355–362. `https://doi.org/10.1016/s1097-2765(04)00210-2`

124. van Oene MM, Dickinson LE, Pedaci F, et al. (2015) Biological magnetometry: torque on superparamagnetic beads in magnetic fields. *Phys Rev Lett* 114: 218301. `https://doi.org/10.1103/PhysRevLett.114.218301`

125. Normanno D, Capitanio M, Pavone FS (2004) Spin absorption, windmill, and magneto-optic effects in optical angular momentum transfer. *Phys Rev A* 70: 053829. `https://doi.org/10.1103/PhysRevA.70.053829`

126. Bikard D, Loot C, Baharoglu Z, et al. (2010) Folded DNA in action: hairpin formation and biological functions in prokaryotes. *Microbiol Mol Biol Rev* 74: 570–588. `https://doi.org/10.1128/MMBR.00026-10`

127. Adhikari AS, Chai J, Dunn AR (2012) Multiplexed single-molecule force proteolysis measurements using magnetic tweezers. *J Vis Exp* 65: e3520. `https://doi.org/10.3791/3520`

128. Johnson KC, Clemmens E, Mahmoud H, et al. (2017) A multiplexed magnetic tweezer with precision particle tracking and bi-directional force control. *J Biol Eng* 11: 1–13. `https://doi.org/10.1186/s13036-017-0091-2`

129. Kuijpers L, van Laar T, Janissen R, et al. (2022) Characterizing single-molecule dynamics of viral RNA-dependent RNA polymerases with multiplexed magnetic tweezers. *STAR Protoc* 3: 101606. `https://doi.org/10.1016/j.xpro.2022.101606`

130. De Vlaminck I, Henighan T, van Loenhout MT, et al. (2012) Magnetic forces and DNA mechanics in multiplexed magnetic tweezers. *PloS One* 7: e41432. `https://doi.org/10.1371/journal.pone.0041432`

131. Ostrofet E, Papini FS, Dulin D (2018). Author correction: Correction-free force calibration for magnetic tweezers experiments. *Sci Rep* 8: 15920. `https://doi.org/10.1038/s41598-018-36219-0`

132. Dulin D, Cui TJ, Cnossen J, et al. (2015) High spatiotemporal-resolution magnetic tweezers: Calibration and applications for DNA Dynamics. *Biophys J* 109: 2113–2125. `https://doi.org/10.1016/j.bpj.2015.10.018`

133. Huhle A, Klaue D, Brutzer H, et al. (2015) Camera-based three-dimensional real-time particle tracking at kHz rates and ångström accuracy. *Nat Commun* 6: 5885. `https://doi.org/10.1038/ncomms6885`

134. Celedon A, Nodelman IM, Wildt B, et al. (2009) Magnetic tweezers measurement of single molecule torque. *Nano Lett* 9: 1720–1725. `https://doi.org/10.1021/nl900631w`

135. Janssen XJ, Lipfert J, Jager T, et al. (2012) Electromagnetic torque tweezers: a versatile approach for measurement of single-molecule twist and torque. *Nano Lett* 12: 3634–3639. `https://doi.org/10.1021/nl301330h`

136. Bessalova V, Perov N, Rodionova V (2016) New approaches in the design of magnetic tweezers–current magnetic tweezers. *J Magn Magn Mater* 415: 66–71. `https://doi.org/10.1016/j.jmmm.2016.03.038`

137. de Vries AH, Krenn BE, van Driel R, et al. (2005) Micro magnetic tweezers for nanomanipulation inside live cells. *Biophys J* 88: 2137–2144. `https://doi.org/10.1529/biophysj.104.052035`

138. Wang J, Wang X, Sun Y (2023) Cellular mechanical measurement by magnetic micro/nanorobots. *Robotics for Cell Manipulation and Characterization*, 71–288, Academic Press. `https://doi.org/10.1016/B978-0-323-95213-2.00012-0`

139. Zhang Z, Huang K, Menq CH (2010) Design, implementation, and force modeling of ouadrupole magnetic tweezers. *IEEE/ASME T Mechatron* 15: 704–713. `https://doi.org/10.1109/TMECH.2009.2032179`

140. Wang X, Ho C, Tsatskis Y, et al. (2019) Intracellular manipulation and measurement with multipole magnetic tweezers. *Sci Robot* 4: eaav6180. `https://doi.org/10.1126/scirobotics.aav6180`

141. Gaire S, Fabian Jr RL, Adhikari R, et al. (2023) Micromechanical study of hyperacetylated nucleosomes using single molecule transverse magnetic tweezers. *Int J Mol Sci* 24: 6188. `https://doi.org/10.3390/ijms24076188`

142. Peterson CL, Laniel MA (2004) Histones and histone modifications. *Curr Biol* 14: R546–R551. `https://doi.org/10.1016/j.cub.2004.07.007`

143. McAndrew CP, Tyson C, Zischkau J, et al. (2016) Simple horizontal magnetic tweezers for micromanipulation of single DNA molecules and DNA-protein complexes. *BioTechniques* 60: 21–27. `https://doi.org/10.2144/000114369`

144. Arya G, Zhang Q, Schlick T (2006) Flexible histone tails in a new mesoscopic oligonucleosome model. *Biophys J* 91: 133–150. `https://doi.org/10.1529/biophysj.106.083006`

145. Arya G, Schlick T (2006) Role of histone tails in chromatin folding revealed by a mesoscopic oligonucleosome model. *Proceedings of the National Academy of Sciences of the United States of America* 103: 16236–16241. `https://doi.org/10.1073/pnas.0604817103`

146. Cherstvy AG, Everaers R (2006) Layering, bundling, and azimuthal orientations in dense phases of nucleosome core particles. *J Phys: Condens Matter* 18: 11429. `https://doi.org/10.1088/0953-8984/18/50/003`

147. Cherstvy AG, Teif VB (2014) Electrostatic effect of H1-histone protein binding on nucleosome repeat length. *Phys Biol* 11: 044001. `https://doi.org/10.1088/1478-3975/11/4/044001`

148. Long X, Parks JW, Stone MD (2016) Integrated magnetic tweezers and single-molecule FRET for investigating the mechanical properties of nucleic acid. *Methods* 105: 16–25. `https://doi.org/10.1016/j.ymeth.2016.06.009`

149. De Vlaminck I, Dekker C (2012) Recent advances in magnetic tweezers. *Annu Rev Biophys* 41: 453–472. `https://doi.org/10.1146/annurev-biophys-122311-100544`

AIMS Press